Available online at www.sciencedirect.com
SCIENCE DIRECT®
Chemical Physics Letters 380 (2003) 223–229
CHEMICAL PHYSICS LETTERS
www.elsevier.com/locate/cplett

Nonlinear light transmission through oxide-protected Au and Ag nanoparticles: an investigation in the nanosecond domain

M. Anija [a], Jinto Thomas [a], Navinder Singh [a], A. Sreekumaran Nair [b], Renjis T. Tom [b], T. Pradeep [b,*], Reji Philip [a,*]

[a] *Raman Research Institute, C.V. Raman Avenue, Bangalore 560 080, India*
[b] *Department of Chemistry and Regional Sophisticated Instrumentation Centre, Indian Institute of Technology Madras, Chennai 600 036, India*

Received 21 May 2003; in final form 2 September 2003
Published online: 26 September 2003

Abstract

Stable Au and Ag nanoparticles protected with TiO_2, ZrO_2, and SiO_2 shells show saturable absorption when excited with moderately energetic nanosecond pulses at 532 nm, but exhibit strong optical limiting at higher intensities. The behavior is explained in terms of the induced optical nonlinearity and nonlinear light scattering. The inherent stability of the core–shell structure renders a high laser damage threshold to these materials, making them promising candidates for high energy optical limiting.

1. Introduction

Core–shell metal nanoparticles is an emerging and active area of current research [1]. There has been a slow but steady growth of activity on nanomaterials with oxide shells [2,3], even though most of the research in this area has been on noble metal nano-cores and molecular shells. Monolayers anchored onto metal cores have been used as precursors to make oxide shells [4,5], but the monolayer route to oxide-shell materials is rather involved requiring multi-step processes and scale-up is difficult. Therefore, we have used a one-step method using the well-known reduction of noble metals with dimethyl formamide (DMF) in the presence of oxide forming precursors [6,7] to synthesize particles of $Au@TiO_2$, $Au@ZrO_2$, $Au@SiO_2$, $Ag@TiO_2$ and $Ag@ZrO_2$ in the size range of 30–60 nm [8]. Interest in such clusters stems from the fact that oxide protection is one way to make metal nanoparticles stable under extreme conditions. For example, our previous work on the optical nonlinearity of ligand-protected metal nanoclusters has shown that they are very good optical limiters [9], but they can be chemically unstable due to ligand desorption. On the other hand, even after irradiating the present

* Corresponding author: Fax: +91-80-361-0492.
E-mail addresses: pradeep@iitm.ac.in (T. Pradeep), reji@rri.res.in (R. Philip).

0009-2614/$ - see front matter © 2003 Elsevier B.V. All rights reserved.
doi:10.1016/j.cplett.2003.09.023

oxide-protected clusters with laser pulses of fluences up to 20 J cm^{-2} and intensities up to 2.8 GW cm^{-2}, no signs of damage were observed. Protection by shells also makes it possible to prepare materials in the form of thin films and disks for diverse applications.

Particles with oxide shells are interesting for other reasons as well. The catalytic properties of oxide surfaces in the presence of the metal core can be important [10,11]. Modified properties such as electrical transport upon exposure to gases and ions are important aspects. The shell being inert can be used to deliver metal clusters into reactive environments and can even be thought of as a mode to deliver drugs [12]. The possibility of removing the core by appropriate chemistry will leave behind a shell, and the chemistry of such nano bubbles will be interesting [13].

In this Letter, we discuss features of nonlinear optical transmission observed in the clusters $Ag@ZrO_2$, $Au@SiO_2$, $Au@ZrO_2$ and $Au@TiO_2$ suspended in 2-propanol, when excited with nanosecond laser pulses at 532 nm. Results show that the samples have a high laser damage threshold and can be used either as saturable absorbers or optical limiters in the appropriate laser fluence regimes.

2. Experimental

The procedure for the synthesis of $Au@TiO_2$, $Au@ZrO_2$ and $Ag@ZrO_2$ particles has been described in the literature [8]. Briefly, the method involves the reduction of Au^{3+} or Ag^{+} by dimethyl formamide in the presence of oxide forming precursors, titanium isopropoxide and zirconium (IV) propoxide. The precursors were hydrolyzed slowly, the process was retarded by the presence of acetylacetone. $Au@SiO_2$ particles were synthesized by the procedure reported earlier [14]. Here, preformed nanoparticles of gold were slowly covered with silica, from an active silica solution prepared from orthosilicate. The particles were collected by centrifugation, washed and resuspended in 2-propanol. Dilute solutions were stable for extended periods. However, higher concentrations tend to coagulate, if stored for periods greater than one week. As the particle characterization has been reported earlier [8,14], we shall outline only the optical nonlinearity in this Letter.

Fig. 1A shows the absorption spectra of various core–shell nanoparticles. For $Ag@ZrO_2$ the plasmon absorption maximum is at 421 nm. The shift of the peak from 400 nm (absorption maximum of bare nanoparticles) is due to the dielectric cover surrounding the cluster [8]. The plasmon absorption maxima of $Au@ZrO_2$ and $Au@SiO_2$ are at 527 and 533 nm, respectively. The absorption peak shifts depending on the shell thickness [8,14]. The transmission electron micrograph of $Ag@ZrO_2$ given in Fig. 1B shows that the average particle size is 50 nm while the typical shell thickness is 3 nm. It must be noted that the shell covers the

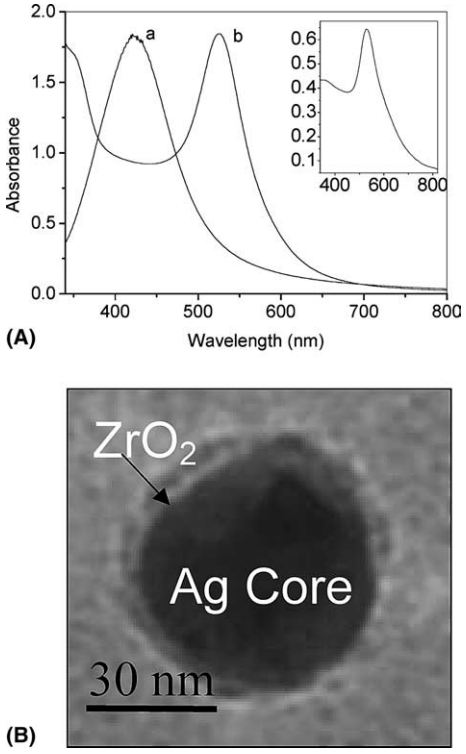

Fig. 1. (A) The optical absorption spectrum of $Ag@ZrO_2$ (a), $Au@ZrO_2$ (b) and $Au@SiO_2$ (inset) nanoparticles. The absorption spectrum peaks at 421 nm for $Ag@ZrO_2$. For $Au@ZrO_2$ and $Au@SiO_2$, the peak maxima are at 527 and 533 nm, respectively, for a 3 nm shell thickness. (B) The transmission electron micrograph of $Ag@ZrO_2$. A ZrO_2 shell of about 3-nm thickness is seen in the TEM.

core completely. The TEM of $Au@ZrO_2$ particles was similar [8]. For $Au@SiO_2$ the Au core was of 10–15 nm diameter while the shell was of about 4-nm thickness [14]. Microscopy did not reveal the presence of free particles of metals or oxides.

To investigate the transmission properties of the nanoparticles, we used 7 ns (FWHM) pulses from a Q-switched Nd:YAG laser emitting at the second harmonic wavelength of 532 nm (2.33 eV). From actual beam profile measurements using the knife-edge method, the spatial intensity profile of the laser is found to be near gaussian. The intensity dependent transmission is measured using an open aperture z-scan [15] set-up, which is automated. In the z-scan, the laser beam is focused using a lens, and the sample is translated along the beam axis (z-axis) through the focal region over a length, several times that of the confocal distance. At each position z the sample sees a different laser fluence, and the position dependent (i.e., fluence dependent) transmission is measured using a pyroelectric energy probe placed after the sample. The focal beam spot size is measured to be 20 ± 2 m in our experiment. By running the laser flash lamps at full power, the pulse to pulse energy stability is improved to better than $\pm 5\%$; these small fluctuations are nevertheless accounted for by using a reference energy probe. Energy reaching the sample is appropriately reduced using neutral density filters. For each z position, five shots are fired at 2-s intervals and the average transmission value is calculated. Using an adaptive algorithm, readings are taken at z intervals of 25 μm around the focal region, which evenly increases to 250 μm at the extreme wings of the z-scan curve. In this way the time taken for each z-scan could be considerably reduced without losing precision.

3. Results and discussion

Since the nonlinear behavior exhibited by the samples was found to be somewhat similar, $Au@SiO_2$ and $Ag@ZrO_2$ were studied in greater detail as representative samples. Figs. 2a and b show the z-scan curves obtained for $Au@SiO_2$ suspended in 2-propanol at various concentrations, for laser energies of 15 and 39 μJ, respectively. Figs. 2c and d depict the corresponding results obtained in the $Ag@ZrO_2$ samples. The z-scans obtained are peculiar in that an increase in transmission is seen at moderate laser fluences,

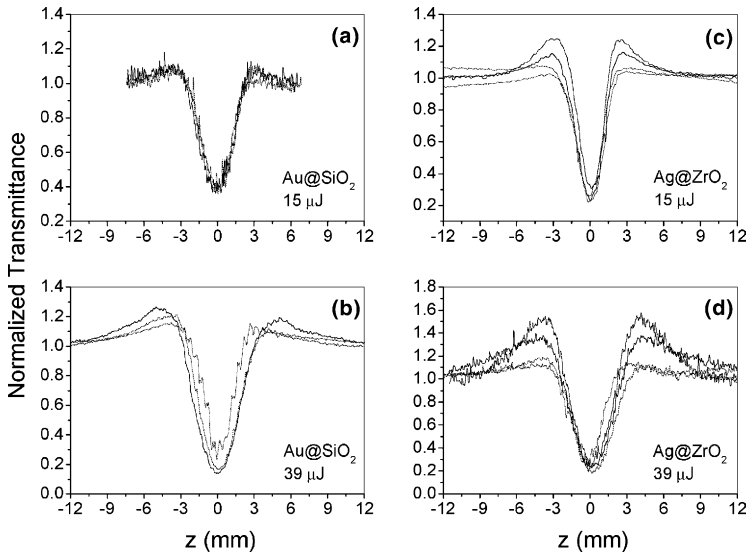

Fig. 2. The z-scan curves obtained for $Au@SiO_2$ and $Ag@ZrO_2$. Laser pulse energies of 15 and 39 μJ are used. Sample linear transmissions at 532 nm are: dash-dotted line – 0.38, solid line – 0.48, dashed line – 0.58, and dotted line – 0.68.

while the transmission drastically decreases at higher fluences. We had earlier observed a similar behavior in thiol-protected nanoparticles suspended in toluene [9]. The increase in transmission is more pronounced at higher concentrations as seen from Fig. 3, in which the z-scans obtained for two concentrated suspensions of $Ag@ZrO_2$ for 5 μJ pumping are shown. The normalized transmittance as a function of the incident laser fluence is shown in Fig. 4, for all samples. The samples have been irradiated up to a fluence of 20 J cm^{-2} without any signs of laser-induced damage.

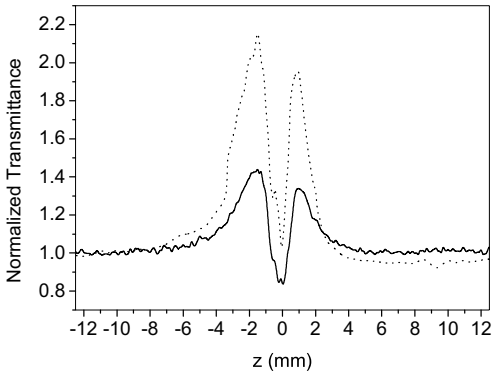

Fig. 3. The z-scans obtained for concentrated suspensions of $Ag@ZrO_2$ in 2-propanol. Linear transmission is 0.2 for the dotted line and 0.3 for the solid line. Laser pulse energy is kept low at 5 μJ.

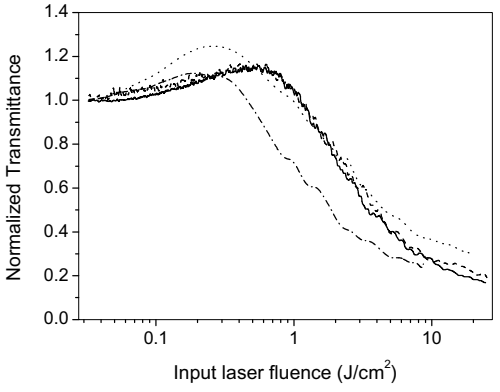

Fig. 4. Normalized transmittance of the particles suspended in 2-propanol, as a function of the input laser fluence at 532 nm. Linear transmission is 0.58 for all samples. Dashed line – $Ag@ZrO_2$, solid line – $Au@SiO_2$, dotted line – $Au@TiO_2$, and dash-dotted line – $Au@ZrO_2$.

To explain these results, it may be noted that for noble metals, in particular gold, the optical properties are determined by the d and s–p (conduction) band electrons. The outermost d and s electrons of the constituent atoms together form a total of six bands, with five of them (the d bands) fairly flat and lying a few eV below the Fermi level, while the sixth band (the s–p band) is almost free electron-like: roughly parabolic with an effective mass very close to that of an electron. Another characteristic feature of metal nanoparticles is the existence of surface plasmons, which are collective electronic excitations at the interface between the metal and the surrounding dielectric. Mie theory [16] attributes the plasmon absorption band of spherical particles to dipolar oscillations of free electrons in the conduction band occupying energy states close to the Fermi energy. The expression for plasmon absorption is given as $(18\pi NVn_0^3/\lambda)\varepsilon_2/((\varepsilon_1+2n_0^2)^2+\varepsilon_2^2)$, where N is the particle number density, V is their volume, n_0 is the refractive index of the medium, and ε_1 and ε_2 are the real and imaginary parts of the metal's dielectric response ε_m. The absorption peak occurs when $\varepsilon_1+2n_0^2=0$, and the absorption bandwidth and plasmon damping are directly related to ε_2.

The observed evolution of fluence dependent transmission from normal to reduced values through an enhanced regime may now be examined on the basis of the pertinent phenomena of Kerr nonlinearity and photoinduced nonlinear light scattering in nanoparticles. Flytzanis and coworkers [17] have shown that there are three major electronic contributions to the Kerr nonlinearity. The first one, $\chi^{(3)}_{\text{intra}}$, is derived from the intra-band conduction electrons in the s–p band. It is electric dipole in nature, originates totally due to the confinement of the free electrons, and is strongly size dependent. The second is from inter-band transitions between the d-bands and the conduction band which occurs when the photon energy is larger than a gap energy, $E_g=\hbar\omega_g$ (which is 1.7 eV for gold, corresponding to the X point of the first Brillouin zone). Inter-band transitions can saturate leading to a mostly imaginary and negative $\chi^{(3)}_{\text{inter}}$, and this contribution is size and shape independent down to very small sizes of about 2.5 nm. The third and most important contribu-

tion $\chi^{(3)}_{sp}$ arises from surface plasmons. By photo-exciting the plasmon band, conduction electrons can be easily elevated to temperatures of several hundred degrees as their specific heats are very small [18,19]. It takes a few picoseconds for these electrons to thermalize with the lattice. During this time, the Fermi–Dirac electron distribution is modified, since part of the one-electron levels below the Fermi level is emptied and part of those above is occupied. This leads to a modification of the dielectric constant ε_m, and the main contribution to the incremental $\delta\varepsilon_m$ will be from those states in the Brillouin zone for which the energy difference between the Fermi level and the d-bands is close enough to the excitation energy. For gold, at the photon energy of 2.33 eV, this comes from the L point of the Brillouin zone for which the gap is $\hbar\omega'_g \cong 2.4$ eV (the X point contributes only weakly to $\delta\varepsilon_m$ since the corresponding gap of 1.7 eV is much smaller). Writing $\varepsilon_m = \varepsilon_X + \varepsilon_L + \varepsilon_D$, where ε_D is the Drude contribution of the free electrons and ε_X and ε_L are components of ε_{inter} with the suffixes denoting the X and L points of the Brillouin zone, respectively, we have $\delta\varepsilon_m \cong (\partial\varepsilon_L/\partial T)\delta T$, where δT is the change in temperature of the free electrons. This modification of ε_m results in a transient re-distribution of the equilibrium plasmon band: the absorption around the peak is reduced and that at the wings is increased. This reduction in absorption is generally referred to as 'plasmon band bleach' in literature [20,21]. In the present case, we see this bleach in the form of humps flanking the valley in the z-scan curves. Even though in Ag the plasmon peak is around 421 nm, we still see the bleach as far as at the excitation wavelength of 532 nm. As for the nonlinear susceptibility values, calculations show that the surface plasmon contribution $\chi^{(3)}_{sp}$ to $\chi^{(3)}_m$ is mainly imaginary, and is larger in magnitude than $\chi^{(3)}_{intra}$ and $\chi^{(3)}_{inter}$. Four-wave mixing experiments have shown that at 2.33 eV, values of $\chi^{(3)}_{sp}$, $\chi^{(3)}_{inter}$ and $\chi^{(3)}_{intra}$ are in the order of 10^{-7}, 10^{-8} and 10^{-10} esu, respectively, for 10 nm diameter gold particles dispersed in silicate glass [18].

The shift to a substantially reduced transmission at higher laser fluences merits special attention because it renders practical applicability to the nanoclusters as optical limiters. Since this limiting is seen only at higher intensities and the excitation is by nanosecond pulses, we may consider the possibility of nonlinear scattering here. Scattering is a fundamental display of light–matter interaction resulting from inhomogeneities in the refractive index, leading to a decrease of net transmission through the medium. Resonant excitation with nanosecond and longer pulses can result in thermally induced transient refractive index changes given by $\Delta n_0 = (dn_0/dt)F_0\alpha/2\rho C_v$, where dn_0/dt is the thermo-optic coefficient, F_0 is the fluence, ρ is the density and C_v is specific heat at constant volume. Such nonlinear scattering contributes to optical limiting in a number of materials, including carbon black [22] and nanotube [23] suspensions, and metal-dendrimer nanocomposites [24]. From comparative studies in gold clusters of 5 and 30 nm average diameters, Mostafavi and co-workers [25] have suggested that the nanosecond limiting in these samples may be explained in the framework of nonlinear scattering. Our own previous studies in thiol-capped Ag, Au and Ag–Au alloy nanoclusters had revealed that for the same laser fluence, nanosecond limiting is more efficient than picosecond limiting [26]. Therefore, to investigate the possibility of nonlinear scattering in the present samples, we did a few z-scans in which a photomultiplier tube (PMT) was used in addition to the existing detectors, to record the scattered radiation. The PMT was maintained at a radial distance of 5 cm from the beam axis. By mounting the sample and PMT on the same translation stage, it was ensured that the PMT is at the same distance of 11 cm from the sample throughout the scan. The typical result obtained is shown in Fig. 5. It is seen that the onset of limiting is marked by a complementary increase in scattering, and the point of maximum limiting coincides with that of maximum scattering. For further confirmation we took photographs of the transmitted beam using a CCD camera. When the sample was away from focus the beam preserved its shape, whereas when it was close to the focus ring-like patterns of scattered light could be seen around the central spot. These observations confirm the significant role of nonlinear scattering in the optical limiting behavior of our samples. To estimate the strength of this nonlinearity, we numerically evaluate the quantity β

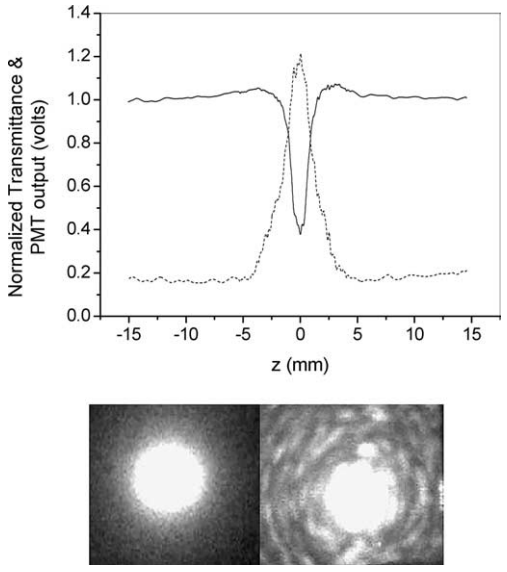

Fig. 5. Nonlinear scattering in the metal nanoparticle suspensions. Solid line in the graph is the normalized transmittance for an Au@SiO_2 sample, while the dashed line is the corresponding scattering from the sample. The points of maximum limiting and maximum scattering coincide. Photographs show the transmitted beam when the sample is away from beam focus (left) and close to the focus (right).

by fitting the z-scan curves to the transmission equation [15]

$$T(z) = [1/\pi^{1/2} q(z)] \int_{-\infty}^{+\infty} \ln[1 + q(z)\exp(-\tau^2)]\,\mathrm{d}\tau$$

with $q(z) = \beta I_0 L/[1 + (z/z_0)^2]$, where I_0 is the peak intensity at the focal point, $L = [1 - \exp(-\alpha l)]/\alpha$, where l is the sample length and α is the linear absorption coefficient, and $z_0 = \pi\omega_0^2/\lambda$ is the Rayleigh range, where ω_0 is the beam waist radius at focus and λ is the light wavelength. β in the present context represents nonlinear scattering that leads to a reduction in transmission: depending on the material under study, it can signify phenomena like two-photon absorption [15] or reverse saturable absorption [27]. To do the fitting we chose only those z-scans obtained at a pump energy of 39 μJ in samples having a linear transmission of 0.48. The equation fits well in the valley region of the curves where limiting occurs, and in the wings where saturable absorption prevails the fit diverges from experimental points as expected. The β values have been calculated to be in the order of 10^{-10} m W^{-1} which indicates a substantial nonlinearity, and these values are comparable to those found for metal-chalcogenide clusters [28,29] and C_{60} solutions [27].

Before closing this discussion, the possibility of photofragmentation in metal nanoclusters also has to be mentioned. Formation of photogenerated, strongly absorptive transient intermediate species has been reported in silver bromide nanoparticles in nanosols [30] and suspended silver-containing nanoparticles [31]. Moreover, Kamat et al. [21] have specifically assigned the strong, broadband transient absorption observed in colloidal silver particles of 40–60 nm diameter to a transient state generated by the photoejection of electrons from the parent cluster. They found that this charge separation leads to the break-up of clusters to form smaller particles (photofragmentation). However, since the plasmon band intensity increases with particle size in the size range of our interest [16,20], photofragmentation should lead to an increase in the linear transmission value. In fact, we found this to happen in just one of the various Ag@ZrO_2 samples we studied: before the experiment the linear transmission was 0.58 and afterwards it was 0.77. On the other hand, Ag@ZrO_2 samples prepared in the other batches as well as the other samples studied were very stable. Therefore, from the several measurements we carried out, we draw the conclusion that the samples we prepared do not normally undergo photofragmentation at the laser fluences used. This encourages us to investigate in more detail the exact mechanism of energy transport, i.e., how the free electrons communicate with the insulator shell, as there are no empty states to populate. Plasmon damping and electron–phonon scattering at the interface may be important, and more studies in particles of varying average sizes would be required to formulate a comprehensive understanding of the energy transport mechanism.

4. Conclusion

Oxide-protected stable particles of Au and Ag have been synthesized and their nonlinear optical transmission measured. It is found that these

samples show either saturable absorption or optical limiting at 532 nm excitation, depending on the applied laser fluence. This behavior is explained in terms of the electronic Kerr nonlinearity and nonlinear scattering in the nanoparticles. The samples have been subjected to laser fluences up to 20 J cm^{-2} and intensities up to 2.8 GW cm^{-2}, and no appreciable signs of laser-induced damage have been observed. The high laser damage thresholds of oxide-protected metal nanoparticles are a promising step towards the realization of nanomaterial based optical limiters.

Acknowledgements

T.P. is grateful to the Ministry of Information Technology, Government of India for funding a research program on optical limiting in nanomaterials. R.P. acknowledges helpful discussions with Profs. N. Kumar and R. Srinivasan during the course of this work.

References

[1] C.-J. Zhong, M.M. Maye, Adv. Mater. 13 (2001) 1507.
[2] P.-S.M. Danek, K.F. Jensen, C.B. Murray, M.G. Bawendi, Chem. Mater. 8 (1996) 173.
[3] B.O. Dabbousi, J. Rodriguez-Viejo, F.V. Mikulec, J.R. Heine, H. Mattoussi, R. Ober, K.F. Jensen, M.G. Bawendi, J. Phys. Chem. B 101 (1997) 9463.
[4] T. Ung, L.M. Liz-Marzan, P. Mulvaney, J. Phys. Chem. B 103 (1999) 6770.
[5] L.M. Liz-Marzan, M. Giersig, P. Mulvaney, Langmuir 12 (1996) 4329.
[6] I. Pastoriza-Santos, L.M. Liz-Marzan, Langmuir 15 (1999) 948.
[7] I. Pastoriza-Santos, D.A. Koktysh, A.A. Mamedov, M. Giersig, N.A. Kotov, L.M. Liz-Marzan, Langmuir 16 (2000) 2731.
[8] R.T. Tom, A.S. Nair, N. Singh, M. Aslam, C.L. Nagendra, R. Philip, K. Vijayamohanan, T. Pradeep, Langmuir 19 (2003) 3439.
[9] R. Philip, G. Ravindra Kumar, N. Sandhyarani, T. Pradeep, Phys. Rev. B 62 (2001) 13160.
[10] N. Kakuta, K.H. Park, M.F. Finlayson, A. Veno, A.J. Bard, A. Campion, M.A. Fox, S.E. Webber, J.M. White, J. Phys. Chem. 89 (1985) 3828.
[11] C. Nasr, S. Hotchandani, W.Y. Kim, R.H. Schmehl, P.V. Kamat, J. Phys. Chem. B 101 (1997) 7480.
[12] S.S. Davis, Trends Biotechnol. 15 (1997) 217.
[13] A.S. Nair, R.T. Tom, V. Suryanarayanan, T. Pradeep, J. Mater. Chem. 13 (2003) 297.
[14] T. Ung, L.M. Liz-Marzan, P. Mulvaney, J. Phys. Chem. B 103 (1999) 6770.
[15] M. Sheik-Bahae, A.A. Said, T.M. Wei, D.J. Hagan, E.W. Van Stryland, IEEE J. Quantum Electron. 26 (1990) 760.
[16] G. Mie, Ann. Phys. 25 (1908) 377.
[17] F. Hache, D. Ricard, C. Flytzanis, U. Kreibig, Appl. Phys. A 47 (1988) 347.
[18] G.L. Eesley, Phys. Rev. B 33 (1986) 2144.
[19] R.W. Schoenlein, W.Z. Lin, J.G. Fujimoto, G.L. Eesley, Phys. Rev. Lett. 58 (1987) 1680.
[20] S.L. Logunov, T.S. Ahmadi, M.A. El-Sayed, J.T. Khoury, R.L. Whetten, J. Phys. Chem. B 101 (1997) 3713.
[21] P.V. Kamat, M. Flumiani, G.V. Hartland, J. Phys. Chem. B 102 (1998) 3123.
[22] L.W. Tutt, T.F. Boggess, Prog. Quantum Electron. 17 (1993) 299.
[23] S.R. Mishra, H.S. Rawat, S.C. Mehendale, K.C. Rustagi, A.K. Sood, R. Bandopadhyay, A. Govindaraj, C.N.R. Rao, Chem. Phys. Lett. 317 (2000) 510.
[24] R.G. Ispasoiu, L. Balogh, O.P. Varnavski, D.A. Tomalia, T. Goodson III, J. Am. Chem. Soc. 122 (2000) 11005.
[25] L. Francois, M. Mostafavi, J. Belloni, J.-F. Delouis, J. Delaire, P. Feneyrou, J. Phys. Chem. B 104 (2000) 6133.
[26] R. Philip, S. Mujumdar, H. Ramachandran, G. RavindraKumar, N. Sandhyarani, T. Pradeep, Nonlinear Opt. 27 (2001) 357.
[27] S. Couris, E. Koudoumas, A.A. Ruth, S. Leach, J. Phys. B 28 (1995) 4537.
[28] R. Philip, G. Ravindra Kumar, P. Mathur, S. Ghosh, Chem. Phys. Lett. 313 (1999) 719.
[29] R. Philip, G. Ravindra Kumar, P. Mathur, S. Ghose, Opt. Commun. 178 (2000) 469.
[30] M.R.V. Sahyun, S.E. Hill, N. Serpone, R. Danesh, D.K. Sharma, J. Appl. Phys. 79 (1996) 8030.
[31] Y.-P. Sun, J.E. Riggs, H.W. Rollins, R. Guduru, J. Phys. Chem. B 103 (1999) 77.